Continuous all-optical deceleration and single-photon cooling of molecular beams

A. M. Jayich,[1] A. C. Vutha,[2] M. T. Hummon,[3] J. V. Porto,[4] and W. C. Campbell[1]

[1]*UCLA Department of Physics and Astronomy, Los Angeles, California 90095, USA*

[2]*York University, Department of Physics and Astronomy, Toronto, ON M3J 1P3, Canada*

[3]*NIST and University of Colorado, Boulder, Boulder, Colorado 80309, USA*

[4]*National Institute of Standards and Technology, Gaithersburg, Maryland 20899, USA*

Ultracold molecular gases are promising as an avenue to rich many-body physics, quantum chemistry, quantum information, and precision measurements. This richness, which flows from the complex internal structure of molecules, makes the creation of ultracold molecular gases using traditional methods (laser plus evaporative cooling) a challenge, in particular due to the spontaneous decay of molecules into dark states. We propose a way to circumvent this key bottleneck using an all-optical method for decelerating molecules using stimulated absorption and emission with a single ultrafast laser. We further describe single-photon cooling of the decelerating molecules that exploits their high dark state pumping rates, turning the principal obstacle to molecular laser cooling into an advantage. Cooling and deceleration may be applied simultaneously and continuously to load molecules into a trap. We discuss implementation details including multilevel numerical simulations of strontium monohydride. These techniques are applicable to a large number of molecular species and atoms with the only requirement being an electric dipole transition that can be accessed with an ultrafast laser.

I. INTRODUCTION

Research with ultracold (< 1 mK) atoms has greatly expanded our knowledge of quantum many-body physics [1], precision metrology [2], possible time and space variation of fundamental constants [3], and quantum information science [4]. Ultracold molecules are desirable as a powerful extension of these efforts, but also as a promising starting point for entirely new investigations. The simplest molecules, diatomics, have more internal degrees of freedom than the two constituent atoms. This makes the body-fixed electric dipole moment of polar molecules accessible with laboratory electric fields, and could lead to discoveries and insights exceeding the rich physics explored with atoms. These oriented electric dipoles can be used to generate strong, long-range, anisotropic dipole-dipole interactions [5], creating new quantum simulators [6], and opening new avenues in quantum computation [7], physical chemistry [8–10], and other fields of physics [11]. In analogy with atoms, we anticipate that a method to apply strong optical forces and to cool many types of molecules will be a valuable resource in the emerging field of ultracold molecules.

Historically, a necessary ingredient for optical control of the motion of atoms and molecules has been an effective electronic cycling transition, where spontaneous emission from the excited state populates only the original ground state. Such transitions have been employed with great success in Doppler cooling, Zeeman slowing, magneto-optical trapping, and a host of other techniques that are the first steps in almost every experiment utilizing ultracold atoms [12–15]. Spontaneous decay processes that lead to "dark states" that are excluded from this cycle are present in most atoms, and are ubiquitous in molecules due to their vibrational degree of freedom. One way to circumvent this issue is to apply more lasers to reconnect these dark states to the cycling transition [16]. This approach was recently demonstrated with carefully chosen molecular species [17–19], and shows particular promise as a method to reach the ultracold regime for those species. An unfortunate consequence of the dark state repumping schemes utilized with these molecules is that they reduce the total scattering rate with each additional repump. This can suppress the maximum achievable optical force by one to two orders of magnitude. For the vast majority of molecules, this force reduction is a serious constraint for beam deceleration using Doppler forces, and would result in cumbersome stopping lengths that will limit the cold molecule flux due to transverse spreading, and the need to repump in a Doppler-insensitive manner over a long interaction length.

We present here an alternative solution to the dark state problem that utilizes *stimulated* emission to prevent spontaneous emission into dark states. This process exploits chirped picosecond pulses to deterministically drive the excited molecule back to the original ground state, eliminating the complications due to the multilevel structure of molecules by isolating a two-level system. This results in a conservative force [20–22] that is considerably stronger than the Doppler cooling force. Ultrafast stimulated slowing should be well suited for the deceleration of molecules from demonstrated molecular beam velocities to a full stop in the laboratory. We then discuss how this deceleration technique (as well as most others that have been demonstrated) can be augmented by a single-photon velocity-cooling process that cools the decelerating molecules into a continuous source of cold, trappable molecules. A few-photon trap loading step such as demonstrated by Lu *et al.* [23] may also be added subsequently to compress the position distribution. Molecules that have been slowed or trapped can then potentially be cooled to the ultracold regime through sympathetic [24], evaporative [25], or Doppler cooling. This approach promises to extend the reach of laser cooling to molecules that are considered difficult to directly laser cool—a class that includes many

molecules that are interesting for applications such as precision measurements [26–28] and cold chemistry [8–10].

II. ULTRAFAST LASER DECELERATION FORCE

The ultrafast stimulated slowing we present here derives its mechanical effect from momentum transfer between photons and molecules. The force is generated by the fast repetition of a cycle where the molecules are first illuminated by a "pump pulse" that is followed immediately by a "dump pulse." The pump pulse counterpropagates with respect to the molecular beam, and the absorption of a photon from this pulse reduces each molecule's momentum by $\hbar k$, where $\hbar$ is the reduced Planck constant and k is the wave vector. The molecules are then deterministically driven back to their ground state by a copropagating dump pulse, which stimulates emission from each molecule, removing another $\hbar k$ of forward momentum. This cycle can then be rapidly repeated many times to produce a strong time-averaged continuous deceleration force. Time ordering of the pulses determines the sign of the force, and occasional delays can be used to reinitialize the populations, which happens quite naturally when generating the ultrafast stimulated slowing from a standard ~80 MHz repetition rate ultrafast laser. In the limit that each laser pulse achieves full population transfer, the optical comb tooth structure of the spectrum that arises from interpulse phase coherence becomes irrelevant, and mode locking serves only as a convenient method for producing picosecond pulses. While we propose a variation of this scheme utilizing chirped picosecond pulses, this force has been used with unchirped pulses to deflect molecular [21] and atomic [22,29] beams in the transverse direction. In this mode of operation, it bears some similarity to the bichromatic force [30–32]. This unchirped realization may be regarded as being (in some respects) the polychromatic limit of the bichromatic force [33].

The pulse duration of a few picoseconds is chosen to provide many of the desirable features of this method. Picosecond pulses are much shorter than the spontaneous emission lifetime, therefore the delay between absorption and stimulated emission can be made short enough that intervening spontaneous emission is negligible. This fast time scale also results in the ability to repeat the cycle much faster than the spontaneous scattering rate (which limits Doppler cooling), and we estimate below that stopping distances on the order of 1 cm will be attainable. The bandwidth of picosecond pulses is also much larger than Doppler shifts for the entire velocity range from beam velocities to a full stop in the laboratory, which allows the optical force to continuously decelerate all velocity classes in the beam. Further, as we discuss below, ultrafast pulses can be chirped over large frequency ranges with passive optics to enhance the state transfer fidelity via adiabatic rapid passage. Since the bandwidths of picosecond pulses are also much smaller than femto- or attosecond pulses, this allows one to limit undesired single and multiphoton transitions (an important concern with molecules) through frequency selection. Finally, a technological advantage of using ultrafast lasers is that the pulses can be frequency doubled with high efficiency, thereby accessing a large variety of atoms and molecules that includes those with transitions deep in the ultraviolet.

III. ENHANCED FIDELITY THROUGH CHIRPED PULSES

Ultrafast stimulated slowing requires that pulses drive the absorption and stimulated emission events. To repeat the cycle many times, each laser pulse must perform an operation equivalent to a π rotation on the Bloch sphere (a "π pulse") for each molecule in the beam. It is crucial to realize high-fidelity population transfers for a large fraction of the molecular beam to avoid unwanted spontaneous emission and to generate a large deceleration force. The fidelity of population transfer by a transform-limited picosecond pulse will inevitably be less than 1 for a large fraction of molecules in a molecular beam for a host of reasons. The main source of decreased fidelity is the laser's Gaussian spatial profile, causing a Rabi frequency variation across the laser beam's transverse and longitudinal intensity distribution. Shot-to-shot pulse energy variation is also a concern, as is beam-pointing stability and a potential imbalance between the co- and counterpropagating laser beams. Circumventing such sources of population transfer infidelity is necessary if large numbers of molecules are to be decelerated with pulses from a mode-locked laser, as pointed out by Galica *et al.* [33].

Population transfer infidelity can be mitigated by the use of adiabatic rapid passage (ARP) [34,35], where sweeping the laser frequency through resonance can result in nearly 100% transfer fidelity. This technique has been examined for atomic deceleration by Metcalf and co-workers [36–38], who have employed long (multinanosecond) pulses and fast phase modulators to drive ARP [39]. We note here an advantage of using ultrafast lasers, where it is straightforward to "chirp" a transform-limited pulse from an ultrafast laser by applying group delay dispersion (gdd) either with a pair of gratings [40], chirped mirrors, optical fibers [41], or a Gires-Tournois interferometer [42]. A chirped pulse has a time-varying frequency that can sweep over a vast frequency range to drive ARP for all velocity classes simultaneously. This chirp is particularly important for molecules because in a multilevel system the chirped pulses can become state selective despite their large bandwidth [41], effectively reducing the complex molecular structure to a set of two-level systems.

For ARP, it is important to maintain the adiabaticity criterion while sweeping over a wide-enough frequency range to make the transfer robust [35]. Figure 1 shows the results of a numerical calculation of the ARP population transfer fidelity for strontium monohydride (SrH; see inset levels of Fig. 3). We plot the probability of populating the excited state (from an initial ground state) as a function of the laser intensity and the gdd applied to a transform-limited $\tau = 7$ ps Gaussian pulse. The operating point (highlighted with a white diamond in Fig. 1) corresponds to 4 W of average power focused to a spot with an intensity full width at half maximum of 0.3 mm. A grating pulse stretcher [40] spaced by 8.7 m with gratings of 2000 lines/mm can achieve -120 ps^2 of gdd. This creates a high-fidelity laser-molecule interaction volume where variations of the intensity as large as a factor of 2 will have a negligible effect on the population transfer. The calculation shown in Fig. 1 includes 1% of the laser power having undesired polarization to model the effect of inevitable imperfections in the optics. These numerical calculations are used as inputs to the Monte Carlo simulation shown in Fig. 5.
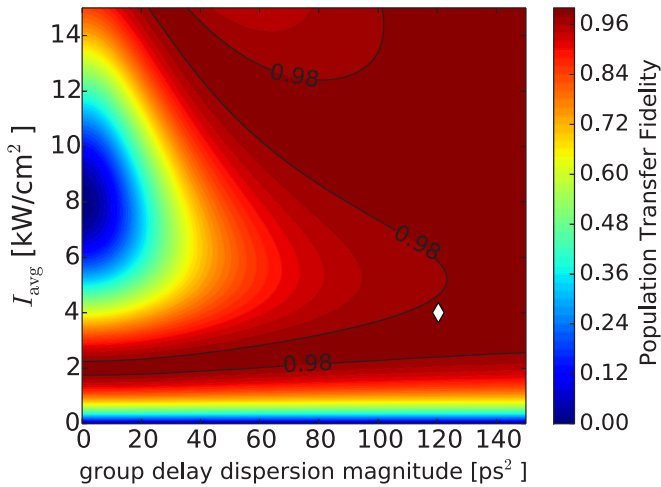
FIG. 1. (Color online) Single-pulse population transfer fidelity for SrH as a function of the time-averaged laser intensity, I_{avg}, and the gdd applied to a $\tau = 7$ ps (temporal) Gaussian transform-limited pulse. The calculated pulse is composed of 99% π-polarized light that connects the two sublevels of an X-state $J = \frac{1}{2}$ manifold to two sublevels of an A-state $J' = \frac{1}{2}$ manifold along a Q-branch. The hyperfine structure is unresolved and therefore not included in the calculation. The white diamond highlights the maximum intensity realized and the gdd used in the Monte Carlo simulation shown in Fig. 5. The typical Rabi flopping as a function of intensity is realized for gdd $= 0$.
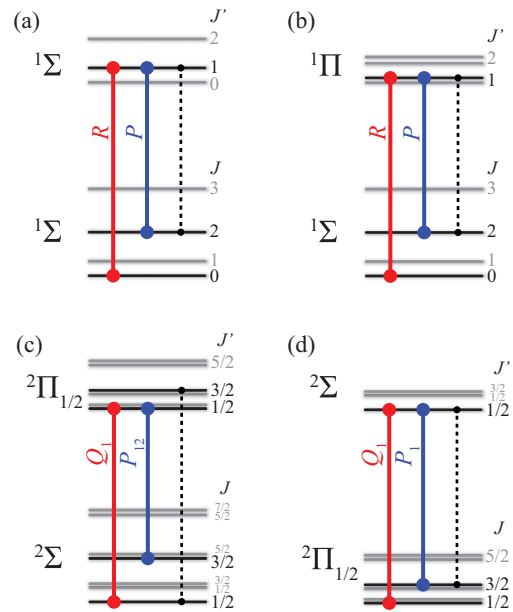

FIG. 2. (Color online) Example schemes for applying ultrafast stimulated slowing to ground-state diatomics. The red lines show the deceleration transition, the blue lines a rotational repump, and the broken black lines indicate the nearest transition that will outcouple molecules from the deceleration cycle if they are significantly within the bandwidth of the pulsed laser. Notable spectroscopically characterized species with these structures include (a) SrO, ThO, (b) AlCl, AlF, (c) SrF, YO, CaF, SrH, and (d) CH, OH, SiF.

IV. MOLECULAR STRUCTURE

For the picosecond-scale pulses considered here, the pulse bandwidth is much larger than hyperfine structure, and we consider only J [N, v, F, and J are good quantum numbers in Hund's coupling case (b), as defined in [43]]. Since each ground quantum state that can be slowed requires a unique excited quantum state for ultrafast stimulated slowing, the number of ground states that can be simultaneously slowed on a given spectroscopic transition is limited to either the multiplicity of the excited or ground state (whichever is smaller). In order to decelerate all of the population in the ground state, it would therefore seem desirable to work on a transition such that these are equal ($J = J'$) by slowing on a Q-branch transition with π-polarized pulses (a prime denotes the excited state). However, for molecules with integer values of J (such as spin singlets and triplets), Q-branch transitions will have dark states even for pure π polarization [44], and an R-branch transition is desirable instead ($J = J' - 1$). We note here that driving a P-branch transition ($J = J' + 1$, as is done for molecular Doppler cooling) could potentially eliminate the need to repump rotational branching, but would come at the cost of dark ground-state sublevels on the pulsed transition, leading to ground-state molecules that do not get decelerated and velocity, position, and optical phase sensitivity that will likely degrade the population transfer fidelity. Slowing on a Q- or R-branch transition may require another laser to rotationally repump molecules that happen to suffer the occasional spontaneous emission event, but this laser may be applied transverse to the molecular beam to avoid Doppler shifts and can be derived from either a pulsed or CW laser.

Every increase in population transfer fidelity reduces the reliance on repump lasers.

Figure 2 shows examples of how the deceleration could be applied to four elementary types of molecular transitions (two singlet and two doublet), though it is generally applicable to any molecule with a strong electronic transition that is accessible to an ultrafast laser. In all of these cases, the pulse bandwidth is limited to be no larger than a few times the rotational constant, which leads to the few picoseconds to tens of picoseconds regime for many diatomic molecules. Even if the unwanted transition is within the laser bandwidth, the ARP process can be made state selective [41] and the unwanted transition can be avoided at the cost of requiring more group delay dispersion to lengthen the pulse chirp in time. Unwanted transitions may be avoided if they are separated from the desired line by at least half of the pulse bandwidth. Numerical calculations confirm that the chirp does not need to be increased substantially from what would be required for robust two-state ARP. Slight polarization imperfections can eventually lead to dark states for molecules decelerated on Q-branch transitions, but we calculate that the polarization purity can easily be maintained at a level where shelving into dark states is not an issue. For this branch the pulse chirp sign can be identical for the pump and dump pulses.

We can make a simple estimate of the distance required to stop the molecular beam from its initial velocity, V_0. For a molecule with mass m and laser repetition rate f_{rep}, we find the stopping distance for perfect fidelity population transfer is

TABLE I. Predicted stopping distances for a molecular beam with initial velocities of 200 and 50 m/s with a laser imparting $2\hbar k$ per laser pulse with $f_{rep} = 80$ MHz. For some of these species the deceleration and repumping level structure is outlined in Fig. 2. It is important to note that for diatomic molecules with rotational constants significantly smaller than the laser pulse bandwidth a more complicated scheme might be required to avoid rotational branching.

Species	Stopping distance (cm) ($V_0 = 200$ m/s)	Stopping distance (cm) ($V_0 = 50$ m/s)	λ (nm)	Mass (amu)	Transition
AlF	0.3	0.02	228	46	$^1\Pi \leftrightarrow {}^1\Sigma$
CaO	1.5	0.10	866	56	$^1\Sigma \leftrightarrow {}^1\Sigma$
CH	0.2	0.01	431	13	$^2\Delta \leftrightarrow {}^2\Pi$
Rb	2.1	0.13	780	85	$^2P_{3/2} \leftrightarrow {}^2S_{1/2}$
SiF	0.7	0.04	439	47	$^2\Sigma \leftrightarrow {}^2\Pi_{1/2}$
SrH	2.1	0.13	751	89	$^2\Pi_{1/2} \leftrightarrow {}^2\Sigma$
TlF	2.0	0.12	284	223	$^3\Pi_0 \leftrightarrow {}^1\Sigma$

given by

$$l_s = \frac{mV_0^2}{4\hbar k f_{rep}}. \tag{1}$$

The stopping distances for several species are given in Table I for $V_0 = 200$ m/s and $V_0 = 50$ m/s with $f_{rep} = 80$ MHz.

V. PHASE-SPACE COMPRESSION

In order to cool the slowed molecules, entropy must be removed. Ultrafast stimulated slowing displaces the momentum distribution, but does not alter its width, and is therefore a deceleration method, not a cooling method. In order to extract entropy from the molecules, we propose to use a continuous-wave (cw) laser to cool the slowed molecules via a single spontaneous emission event. Such single-photon cooling was first demonstrated in 1991 by Cornell, Monroe, and Wieman [45], and has been studied extensively in various forms [23,46–51]. The scheme we describe here can be thought of as the momentum-space equivalent of these position-space ideas, and position-sensitive versions (such as that recently demonstrated for CaF molecules [23]) can be applied with this scheme to complete the phase-space compression in both directions.

Within the framework of ultrafast stimulated slowing, a delay can periodically be inserted after a burst of deceleration cycles during which a collinear cw laser illuminates the molecules. This narrow-band cw laser is tuned to optically pump ground state molecules into a long-lived dark state (such as a different vibrational level) via a single spontaneously emitted photon, where they remain and are no longer addressed by the deceleration laser. The high likelihood of optical pumping of this sort is precisely the issue that makes molecules difficult to laser cool in the first place, but it can be exploited to our advantage to efficiently cool each molecule in a single spontaneous emission event. Since this cw optical pumping step is sensitive to the velocity of the molecules via their Doppler shift, molecules only get pumped into dark states when they reach the desired target velocity. The spontaneous emission of a photon during this optical pumping process heralds the arrival of the molecule into the desired target velocity, thereby extracting entropy from the molecule.

Given a long interaction time with the cw beam, the final velocity width of the optically pumped molecules can in principle be reduced to the recoil limit if the cw laser drives a narrow transition. However, in practice the deceleration rate will set the final velocity width well before the recoil limit is reached. The reason for this is that the molecules must spend enough time in the vicinity of the target velocity to absorb a photon from the cw beam, so larger deceleration rates will require more cw laser power, and power broadening will dictate the addressable velocity width. If the time-averaged force from the ultrafast stimulated slowing (including delays for optical pumping) is given by $F = \hbar k f_{rep}$, a cw velocity-cooling laser of similar wavelength will produce a final velocity distribution with an effective temperature

$$k_B T_{rep} \geqslant 2\pi\hbar f_{rep}, \tag{2}$$

where k_B is the Boltzmann constant. This relationship demonstrates the connection between the deceleration force and the final effective temperature in this scheme.

After their longitudinal momentum space density has been compressed, molecules can be subjected to a similar single-photon cooling step in position space through position-sensitive optical pumping into a trap [23,45,50,52]. In principle, each molecule needs to spontaneously emit only two photons during the entire process from beam to trap, demonstrating the large capacity each spontaneously emitted photon has for carrying away entropy.

VI. APPLICATION TO STRONTIUM MONOHYDRIDE

We have used numerical simulations to investigate the performance of the all-optical deceleration and cooling using ^{88}SrH as a specific example. This molecule is considered for three primary reasons: the $A\,^2\Pi_{1/2} \leftrightarrow X\,^2\Sigma^+$ electronic transition is strong ($\tau = 34$ ns), addressable by a Ti:sapphire laser ($\lambda = 751$ nm), and has a low branching ratio to vibrational dark states (1/67 [16]) which makes it relatively forgiving of population transfer infidelities. The relevant level structure of ^{88}SrH ($A\,^2\Pi_{1/2} \leftrightarrow X\,^2\Sigma^+$) is depicted in Fig. 3. We propose to execute the deceleration cycle with π-polarized light from the X-state $N = 0$, $J = \frac{1}{2}$ manifold to the A-state ($N' = 1$), $J' = \frac{1}{2}$ manifold on the Q_1 branch. These two manifolds have the same number of sublevels ($J = J' = \frac{1}{2}$), as shown in the inset of Fig. 3, and π-polarized light will therefore slow all molecules in the rotational ground state.

To produce rovibrationally cold molecules we envision using a cryogenic buffer-gas beam (CBGB) source, as depicted in Fig. 4, such as those described in [53]. In these CBGB
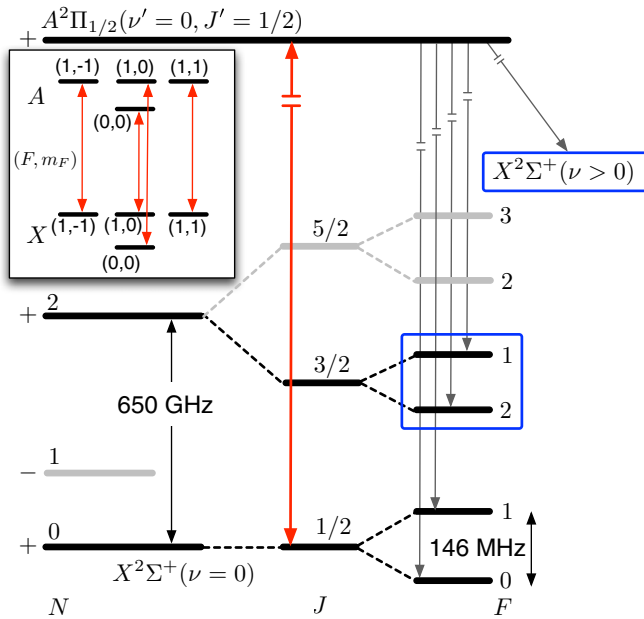
FIG. 3. (Color online) The pertinent level structure for ^{88}SrH. A full slowing cycle can be completed along the Q_1 branch, pictured as an inset, with Zeeman sublevels, m_F, shown driven by π-polarized light. Occasional decays from the excited state will populate the desired slowing state, along with dark states highlighted in blue, including higher vibrational states, which can be repumped with cw or pulsed lasers.

sources, molecules are cooled by collisions with a cold buffer gas (viz., helium or neon), and intense beams with forward velocities as low as 35 m/s [54] have been produced.

Figure 5 shows the computer simulation of the longitudinal phase-space evolution obtained by tracking full three-dimensional molecule trajectories (for a detailed treatment of the simulation parameters see Sec. VII). The black distribution represents the initial beam as it exits the CBGB source, which evolves into the gray distribution in the absence of deceleration and cooling. The blue points show the effect of deceleration by ultrafast pulses and cooling by the cw velocity-cooling laser.
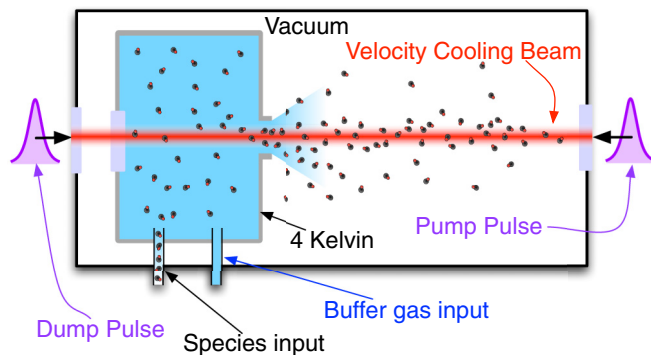

FIG. 4. (Color online) Molecules emitted from a CBGB source are in their rovibrational ground state. After exiting the nozzle they are slowed by picosecond pulses (shown in purple). A velocity-selective optical-pumping laser (red) drives single-photon cooling and compresses the velocity-space density of the beam.

The deceleration translates the distribution toward negative velocity. We simulate deceleration cycle bursts that are each 28 pulses long, interleaved with delay periods of repumping and single-photon cooling. The duration of these delays results in an effective time-averaged repetition rate of $f_{\text{rep}} = 47$ MHz. The single-photon cooling laser was tuned to be resonant with molecules traveling with a longitudinal velocity near 7 m/s. Molecules gather near this target velocity due to the optical pumping process, and the histogram shown on the right side of Fig. 5 shows this density increase on a semilogarithmic scale. We find that molecules with large transverse velocity wander out of the deceleration laser beam and therefore never make it to the target velocity. With the addition of a molecular guide (magnetic or electric), it may be possible to enhance the range of transverse velocities and positions that are captured.

For those molecules that were successfully optically pumped out of the deceleration cycle by the cw velocity-cooling laser (which constitute more than half of those simulated), their momentum was reduced by an average of $36\hbar k$ per spontaneously emitted photon. This value is $1\hbar k$ for traditional laser cooling. This demonstrates the power of ultrafast stimulated slowing to open the door to species with branching ratios tens of times worse than the special Doppler-coolable species. Furthermore, the total distance required for this deceleration is ~ 1 cm, as shown by the x axis of Fig. 5, providing a simplification of the apparatus required to produce cold molecules. We did not numerically simulate the addition of a position-selective optical pumping laser or trap (which has been demonstrated recently with molecules [23]), but we find that the velocity compression alone increased the peak six-dimensional phase-space density by a factor of 16. The average stopping distance for the cooled molecules is 0.4 cm. This agrees reasonably with the simple analytic expression of Eq. (1), which gives 0.2 cm with $f_{\text{rep}} = 47$ MHz (the effective repetition rate is reduced by the cooling and repumping window).

VII. MONTE CARLO SIMULATION

The numerical simulation presented in Fig. 5 consists of two parts: the molecular beam source and the control lasers. We combine estimates based on current technology for cold molecular beam sources and picosecond lasers to estimate a number of decelerated and cooled SrH molecules (which could be subsequently trapped). We consider a molecular beam with center of mass velocity 50 m/s as in [54], which is realizable for many species [55]. The simulation is performed assuming 4 W of time-averaged laser power at a repetition rate of 80 MHz in 7 ps transform-limited (temporal) Gaussian pulses that are chirped by -120 ps^2 of gdd before interacting with the molecules. The temporal Gaussian is chosen for computational ease, and results with other similar pulse shapes (such as hyperbolic secant) are similar. To determine the population transfer fidelity we calculate the ARP dynamics for a given intensity by time evolving the Schrödinger equation with two ground states and two excited states.

We assume that a single pulse is recycled, e.g., by a mirror, to generate the pump and dump pulses for a deceleration cycle. The probability of population transfer by a chirped pulse is determined by the gdd and the intensity, the latter of which
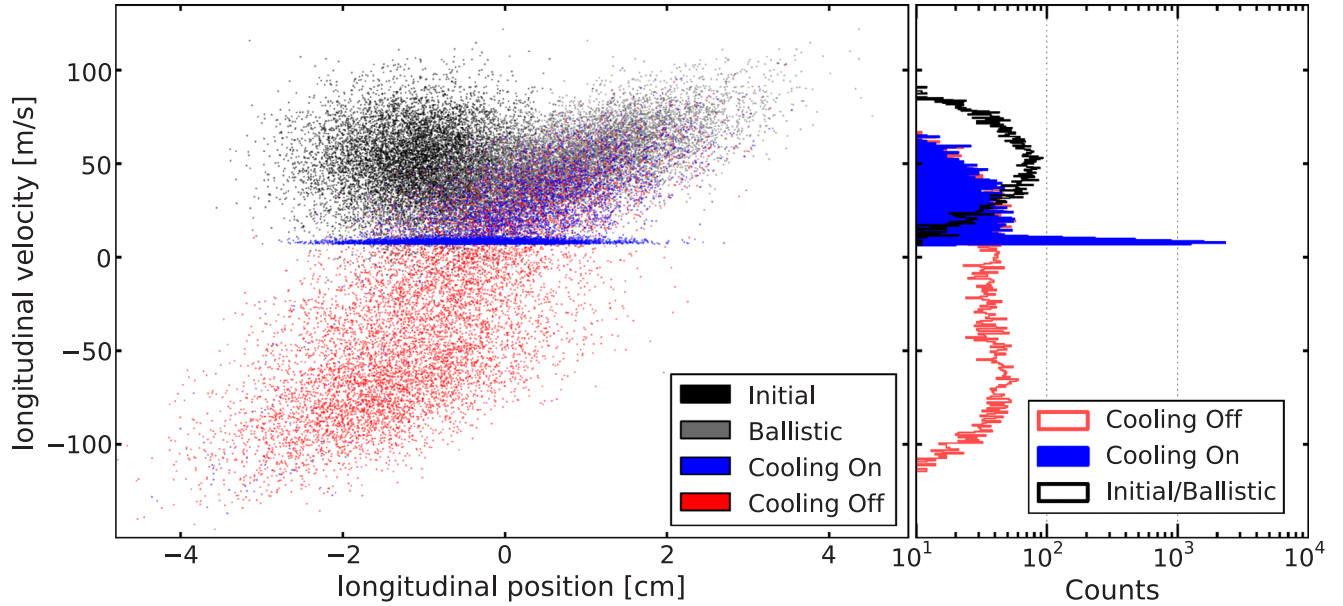
FIG. 5. (Color online) A Monte Carlo simulation of the deceleration and cooling for SrH. The longitudinal phase-space distribution is shown for the initial distribution (black), ballistic trajectories (gray), the trajectories when the ultrafast laser deceleration force is applied (red), and the trajectories when both the deceleration force and single-photon-cooling lasers are applied (blue). A histogram of longitudinal velocities is shown on the right in a semilogarithmic scale.

varies as a function of position. The state of the molecule is not evolved between pump and dump pulses, as this delay can be made essentially as short as the pulse widths, which are negligible compared to the spontaneous emission lifetime. After the deceleration cycle the molecule evolves ballistically for $1/f_{\rm rep}$. During this time if a molecule is left in the excited state (due to bad fidelity) it may decay (every spontaneous decay imparts a momentum kick in a random direction) back to the ground state or to a dark state. The branching to the dark state is given by the combination of the rotational branching to the $N = 2$, $J = 3/2$ manifold (1/3) and to the $v = 1$ states (1/67). Molecules in the dark state are not decelerated. Because of intensity-variation-induced population transfer infidelity, dark state repumping is necessary, and after every 14 deceleration cycles (28 pulses) a repumping (and cooling) step is inserted. We assume that 3/8 of the dark state molecules are repumped to the excited state, from which they can decay again to the ground or dark state with the branching ratios above. The decay probability upon excitation by the repump is near unity because the repumping and cooling window is 125 μs. In order to achieve a low final temperature, it is important to have a long cooling window, as illustrated by Eq. (2). The cooling laser is detuned 9 MHz from the zero velocity class, which corresponds to a forward velocity near 7 m/s. The cooling intensity (0.10 mW/mm^2) is set so that a near π rotation is performed on a $\gamma/2\pi = 1$ MHz transition to an excited state that preferentially decays to a state that is not addressed by the ultrafast laser. During the repumping and cooling window the molecules evolve ballistically. The burst of 14 deceleration cycles (28 total pulses) followed by the 125 μs repumping and cooling window is repeated 1200 times, giving a total of 33 600 deceleration pulses.

Molecules with high transverse velocity will not be significantly decelerated since they will quickly leave the high-

intensity region of space. Therefore we ignore any molecules that have a transverse velocity greater than 0.75 m/s, giving rise to a simulated fraction of $\sim 8 \times 10^{-4}$. We use a diameter of 0.35 mm for the molecular beam source.

For the simulation shown in Fig. 5, the slowing and cooling process captured more than 68% of the molecules. For these cooled molecules, an average of $36\hbar k$ of momentum is transferred per (unwanted) spontaneous decay event. The phase space of the cooled molecules was compressed by a factor of 16.1 (in other simulations with hotter, faster samples the compression factor can be as large as 35). Of the molecules that were cooled 94% are trappable, where a cooled molecule is considered trappable if it is moving <10 m/s and intersects a 1 cm diameter circle that is 2 cm from the source.

VIII. SUMMARY

We have outlined an all-optical scheme to generate trappable, cold molecules that can be applied to a variety of molecules with the only requirement being a transition that can be accessed with ultrafast lasers. This opens up access to a very large number of diatomic molecules, as well as atoms that are not traditionally amenable to laser cooling. Simulations indicate that significant deceleration and cooling are possible with existing technology. The technique presented here has the desirable feature of being all optical, circumventing the need for complex *in vacuo* components for cold molecule generation. For this reason we anticipate that it will be sufficiently flexible to be used in concert with other techniques that have been developed over the past 15 years to produce ultracold molecules [54,56–59]. Finally, we note that another application of this optical force and velocity-cooling process is that it can also be used to *accelerate* a sample of cold atoms or molecules to large velocities and produce narrow distributions. Atomic beams with high spectral luminosity such as this might

be used to explore collisional physics, including narrow shape resonances [60] or to augment atom interferometry [61,62].

ACKNOWLEDGMENTS

[1] I. Bloch, J. Dalibard, and S. Nascimbene, Nat. Phys. **8**, 267 (2012).

[2] C. F. Ockeloen, R. Schmied, M. F. Riedel, and P. Treutlein, Phys. Rev. Lett. **111**, 143001 (2013).

[3] S. N. Lea, Rep. Prog. Phys. **70**, 1473 (2007).

[4] J. J. García-Ripoll, P. Zoller, and J. I. Cirac, J. Phys. B **38**, S567 (2005).

[5] B. Yan, S. A. Moses, B. Gadway, J. P. Covey, K. R. A. Hazzard, A. M. Rey, D. S. Jin, and J. Ye, Nature (London) **501**, 521 (2013).

[6] A. Micheli, G. K. Brennen, and P. Zoller, Nat. Phys. **2**, 341 (2006).

[7] D. DeMille, Phys. Rev. Lett. **88**, 067901 (2002).

[8] R. V. Krems, Phys. Chem. Chem. Phys. **10**, 4079 (2008).

[9] M. T. Bell and T. P. Softley, Mol. Phys. **107**, 99 (2009).

[10] O. Dulieu, R. Krems, M. Weidemuller, and S. Willitsch, Phys. Chem. Chem. Phys. **13**, 18703 (2011).

[11] L. D. Carr, D. DeMille, R. V. Krems, and J. Ye, New J. Phys. **11**, 055049 (2009).

[12] D. J. Wineland, R. E. Drullinger, and F. L. Walls, Phys. Rev. Lett. **40**, 1639 (1978).

[13] S. V. Andreev, V. I. Balykin, V. S. Letokhov, and V. G. Minogin, J. Exp. Theor. Phys. **34**, 442 (1981).

[14] W. D. Phillips and H. Metcalf, Phys. Rev. Lett. **48**, 596 (1982).

[15] E. L. Raab, M. Prentiss, A. Cable, S. Chu, and D. E. Pritchard, Phys. Rev. Lett. **59**, 2631 (1987).

[16] M. D. Di Rosa, Eur. Phys. J. D **31**, 395 (2004).

[17] E. S. Shuman, J. F. Barry, and D. DeMille, Nature (London) **467**, 820 (2010).

[18] V. Zhelyazkova, A. Cournol, T. E. Wall, A. Matsushima, J. J. Hudson, E. A. Hinds, M. R. Tarbutt, and B. E. Sauer, arXiv:1308.0421.

[19] M. T. Hummon, M. Yeo, B. K. Stuhl, A. L. Collopy, Y. Xia, and J. Ye, Phys. Rev. Lett. **110**, 143001 (2013).

[20] A. P. Kazantsev, J. Exp. Theor. Phys. **39**, 784 (1974).

[21] V. S. Voĭtsekhovich, M. V. Danileĭko, V. I. Negriĭko, V. I. Romanenko, and L. P. Yatsenko, J. Exp. Theor. Phys. **59**, 408 (1994).

[22] B. Nölle, H. Nölle, J. Schmand, and H. J. Andrä, Europhys. Lett. **33**, 261 (1996).

[23] H.-I. Lu, I. Kozyryev, B. Hemmerling, J. Piskorski, and J. M. Doyle, arXiv:1310.2669.

[24] C. J. Myatt, E. A. Burt, R. W. Ghrist, E. A. Cornell, and C. E. Wieman, Phys. Rev. Lett. **78**, 586 (1997).

[25] W. Ketterle and N. J. van Druten, *Advances in Atomic, Molecular and Optical Physics* (Academic, New York, 1996), Vol. 37, p. 181.

[26] D. A. Wilkening, N. F. Ramsey, and D. J. Larson, Phys. Rev. A **29**, 425 (1984).

[27] E. A. Hinds, Phys. Scr. **T70**, 34 (1997).

[28] A. C. Vutha, W. C. Campbell, Y. V. Gurevich, N. R. Hutzler, M. Parsons, D. Patterson, E. Petrik, B. Spaun, J. M. Doyle, G. Gabrielse, and D. DeMille, J. Phys. B **43**, 074007 (2010).

[29] A. Goepfert, I. Bloch, D. Haubrich, F. Lison, R. Schütze, R. Wynands, and D. Meschede, Phys. Rev. A **56**, R3354 (1997).

[30] J. Söding, R. Grimm, Y. B. Ovchinnikov, P. Bouyer, and C. Salomon, Phys. Rev. Lett. **78**, 1420 (1997).

[31] L. Yatsenko and H. Metcalf, Phys. Rev. A **70**, 063402 (2004).

[32] M. A. Chieda and E. E. Eyler, Phys. Rev. A **84**, 063401 (2011).

[33] S. E. Galica, L. Aldridge, and E. E. Eyler, Phys. Rev. A **88**, 043418 (2013).

[34] M. M. T. Loy, Phys. Rev. Lett. **32**, 814 (1974).

[35] N. V. Vitanov, T. Halfmann, B. W. Shore, and K. Bergmann, Annu. Rev. Phys. Chem. **52**, 763 (2001).

[36] T. Lu, X. Miao, and H. Metcalf, Phys. Rev. A **71**, 061405 (2005).

[37] T. Lu, X. Miao, and H. Metcalf, Phys. Rev. A **75**, 063422 (2007).

[38] D. Stack, J. Elgin, P. M. Anisimov, and H. Metcalf, Phys. Rev. A **84**, 013420 (2011).

[39] J. Elgin and H. Metcalf, Bull. Am. Phys. Soc. **58** (2013).

[40] E. Treacy, IEEE J. Quantum Electron. **5**, 454 (1969).

[41] J. S. Melinger, S. R. Gandhi, A. Hariharan, J. X. Tull, and W. S. Warren, Phys. Rev. Lett. **68**, 2000 (1992).

[42] J. Kuhl and J. Heppner, IEEE J. Quantum Electron. **22**, 182 (1986).

[43] J. M. Brown and A. Carrington, *Rotational Spectroscopy of Diatomic Molecules* (Cambridge University Press, Cambridge, UK, 2003).

[44] D. J. Berkeland and M. G. Boshier, Phys. Rev. A **65**, 033413 (2002).

[45] E. A. Cornell, C. Monroe, and C. E. Wieman, Phys. Rev. Lett. **67**, 2439 (1991).

[46] C. H. Raymond Ooi, K.-P. Marzlin, and J. Audretsch, Eur. Phys. J. D **22**, 259 (2003).

[47] E. Narevicius, S. T. Bannerman, and M. G. Raizen, New J. Phys. **11**, 055046 (2009).

[48] J. J. Thorn, E. A. Schoene, T. Li, and D. A. Steck, Phys. Rev. A **79**, 063402 (2009).

[49] A. Aghajani-Talesh, M. Falkenau, A. Griesmaier, and T. Pfau, J. Phys. B **42**, 245302 (2009).

[50] J. Riedel, S. Hoekstra, W. Jäger, J. J. Gilijamse, S. Y. T. van de Meerakker, and G. Meijer, Eur. Phys. J. D **65**, 161 (2011).

[51] M. Falkenau, V. V. Volchkov, J. Rührig, A. Griesmaier, and T. Pfau, Phys. Rev. Lett. **106**, 163002 (2011).

[52] J. Stuhler, P. O. Schmidt, S. Hensler, J. Werner, J. Mlynek, and T. Pfau, Phys. Rev. A **64**, 031405(R) (2001).

[53] N. R. Hutzler, H.-I. Lu, and J. M. Doyle, Chem. Rev. **112**, 4803 (2012).

[54] D. Patterson and J. M. Doyle, J. Chem. Phys. **126**, 154307 (2007).

[55] J. M. Doyle (private communication).

[56] H. L. Bethlem, G. Berden, and G. Meijer, Phys. Rev. Lett. **83**, 1558 (1999).

[57] S. A. Rangwala, T. Junglen, T. Rieger, P. W. H. Pinkse, and G. Rempe, Phys. Rev. A **67**, 043406 (2003).

[58] N. Vanhaecke, U. Meier, M. Andrist, B. H. Meier, and F. Merkt, Phys. Rev. A **75**, 031402 (2007).

[59] M. Zeppenfeld, B. G. U. Englert, R. Glockner, A. Prehn, M. Mielenz, C. Sommer, L. D. van Buuren, M. Motsch, and G. Rempe, Nature (London) **491**, 570 (2012).

[60] H. M. J. M. Boesten, C. C. Tsai, J. R. Gardner, D. J. Heinzen, and B. J. Verhaar, Phys. Rev. A **55**, 636 (1997).

[61] S.-w. Chiow, T. Kovachy, H.-C. Chien, and M. A. Kasevich, Phys. Rev. Lett. **107**, 130403 (2011).

[62] J. G. Wacker, Phys. Lett. B **690**, 38 (2010).